

OPTIMAL WATERWAY PASSAGE IN SUBMERGED CURVED DEFLECTOR FOR MINIMIZATION OF LOCAL SCOUR

Abdelazim M. Negm¹, Gamal M. Abdel-Aal², Magid M. Elfiky³,
and Yasser A. Mohamed⁴

¹ Professor of Hydraulics and Vice Dean for Education and Students Affairs,
Faculty of Engineering, Zagazig University, Zagazig, Egypt

E-mail: amnegr85@yahoo.com

^{2,3} Professors of Hydraulics, Water and Water Structures Engineering Dept.,
Faculty of Engineering, Zagazig University, Zagazig, Egypt

⁴ Assistant Professor, Water and Water Structures Engineering Dept.,
Faculty of Engineering, Zagazig University, Zagazig, Egypt

ABSTRACT

Many of the huge structures like New Esna, and New Nega Hammadi Barrages face a great harmful caused by local scour downstream (DS) their stilling basins. It is planned to redesign many of these structures to minimize these harmful impacts of the DS local scour. This research paper presents the results of an extensive experimental investigation on using an optimized submerged curved deflector to efficiently minimize the local scour DS the stilling basin of the multivents regulators. Different percentages of waterway passage through the deflector were tested while the deflector was fixed at an optimized location. The tests were carried out under submerged flow conditions. The main goal of the present research paper is to determine the optimal percentage of waterway passage of the tested deflector. In order to achieve this goal, the effects of flow submergence, Froude number, operation policy of gates and percentage waterway passage of deflector on the maximum scour dimensions (depth and length) and on the velocity distribution near to bed were investigated. It was found that a waterway passage of 28% minimize both the scour dimensions and the near-bed-velocity. An average reduction of 86% in the maximum scour depth and 77% in the near-bed-velocity was obtained when the deflector was fixed at the optimal position.

Keywords: Local scour, Hydraulic structure, Multi-vents Regulators, submerged hydraulic jump, flow deflector.

INTRODUCTION

One major source of problems for the multivents regulators is the DS local scour due to the excessive energy associated with the high velocity of flow issuing under the gates. Hydraulic jump is normally created to act as a natural device to dissipate such energy. Stilling basins are normally designed to control the formation of the hydraulic

jump within the floor length. A comprehensive list of published papers on the hydraulic jumps and stilling basins could be found in Hager [8]. The submerged hydraulic jump was studied by Govinda Rao and Rajaratnam [7], Rajaratnam [18,19], Narayanan and Bhargara [13], Abdelgawad and McCorquodale [2], McCorquodale and Khalifa [11], El-Azizy [6], Long [10], Negm et al. [14] and Abdel-Aal [1]. On the other hand, Zidan et al. [21], Hassan et al. [9] investigated the local scour DS hydraulic structures. Abouel-Atta [3] investigated the scour phenomena due to a radial free hydraulic jump flowing over a rigid diverging apron to an erodible bed. Ali [4] investigated the best location of baffle sill and different variables affected upon the local scour DS hydraulic structures. Mohamed et al. [12] studied the effect of different positions and heights of a continuous sill on scour DS of hydraulic structures. El Masry [5] studied experimentally the effect of a fully angled-baffled apron on the local scour DS a heading-up structure. Saleh et al. [20] studied the effect of asymmetric side sill on maximum scour DS of sudden stilling basins. Negm et al. [15] investigated the effects of operation of gates of multi-vents regulators on flow patterns along the bed via the analysis of the measured velocities near to bed. Also, Negm et al. [16] proved that the symmetric operation scenario of gates reduces the scour dimensions compared to the asymmetric operation of gates.

THEORETICAL ANALYSIS

Dimensional analysis based on Buckingham theory was used to develop functional relationship between the scour depth and the other relevant variables (as shown in Fig. (1)). The functional relationship for the maximum local scour depth, d_s , could be expressed as follows:

$$\frac{d_s}{y_1} = f(S, e, a_o, F_1, \omega) \quad (1)$$

in which, $S=y_t/y_1$ is the submergence ratio, y_t is the tailwater depth, y_1 is the initial depth of perfect clear jump, e is the expansion ratio, $e=B/b_e$, B is the width of the flume, b_e is the effective width of openings, A_o is the relative waterway passage of the circular deflector $A_o=a_o/A_t$, a_o is the area of waterway passage in the deflector, A_t is the total area of the deflector, $F_1 (=v_1/\{gy_1\}^{0.5})$ is Froude number at the vena contracta where the velocity is v_1 , g is the gravitational acceleration and ω stands for the gates operating scenario.

Similarly, the relative maximum near-bed-velocity measured at the end of the basin (v_b) could be expressed as follows:

$$\frac{v_b}{\sqrt{gy_1}} = \psi = f(S, e, a_o, F_1, \omega) \quad (2)$$

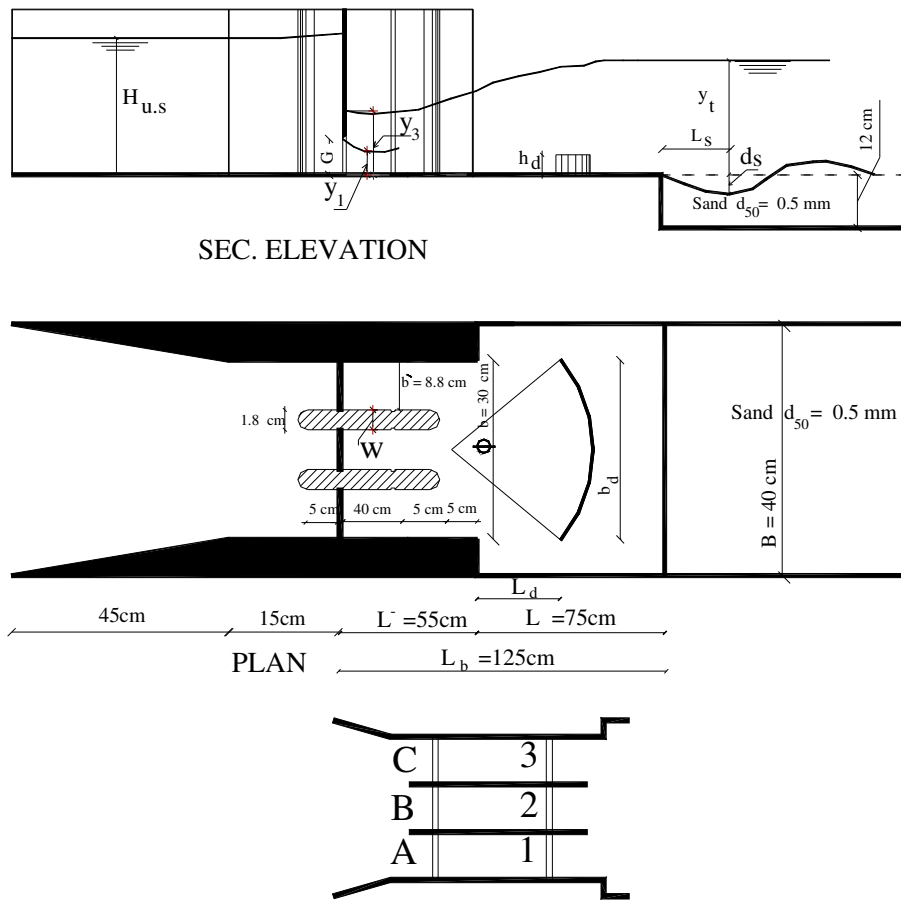


Figure 1 Definition sketch for the tested experimental model

EXPERIMENTAL WORK

Test Flume and Model Details

The experimental work was conducted in the Hydraulic Research Institute (HRI), National Research Center, Ministry of Water Resources and Irrigation, Delta Barrages, Egypt. A re-circulating adjustable flume of 44.1 m long, 60 cm deep and 40 cm wide was used. The flume is equipped with tailgate, sluice gate, depth measuring device, ultrasonic flow meter for discharge measurements. The details and dimensions of the experimental model are shown in Figure 1. The details of the curved deflector are shown in Figure 2. The deflector is fixed at the relative optimal location of $0.06L_b$ from the beginning of the basin as obtained by Negm et al. [17]. The effect of submergence ratio was studied for operating all gates by Negm et al. [15,16]. It was found that the increase of submergence decreases the maximum near-bed-velocity ratio and consequently the relative maximum scour depth was decreased. This is mainly due to the effect of the increasing weight associated with the increase of submergence. Therefore, the effect of submergence ratio which was mentioned in Eqs. (1) and (2) was kept constant. The overall dimensions of the test model (curved

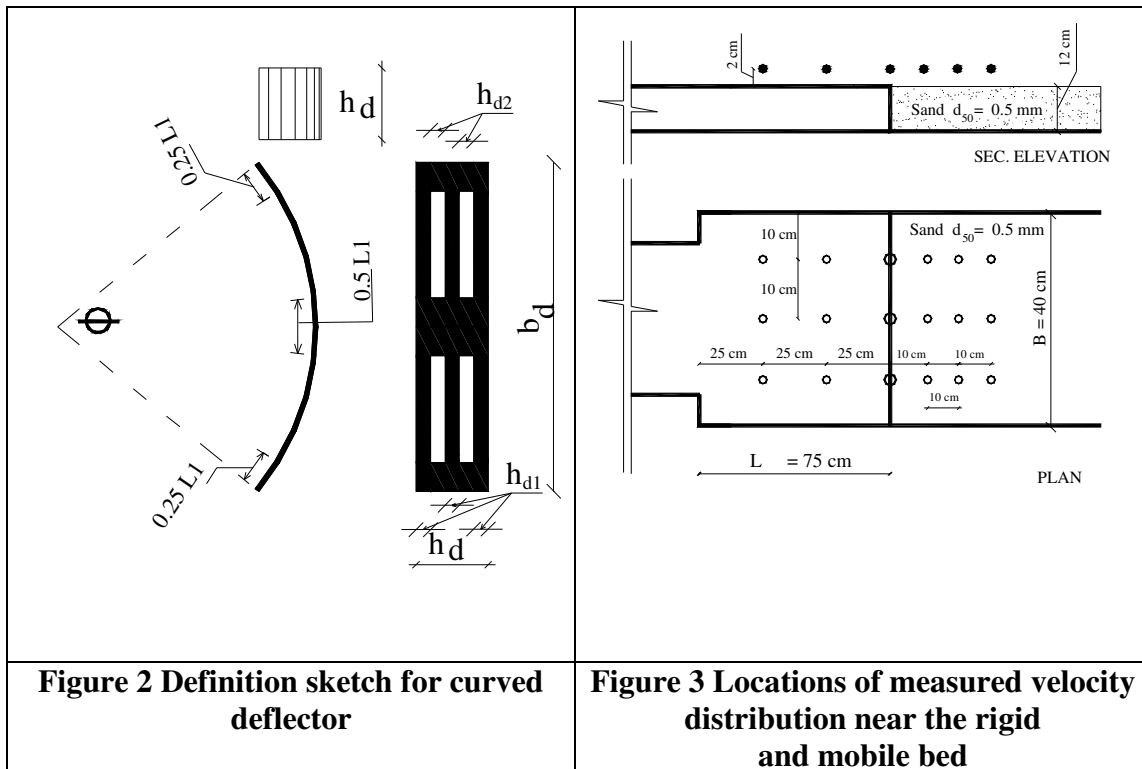
deflector) is ($L_d= 4.5\text{cm}$, $h_d=6.0\text{cm}$, $b_d= 30\text{cm}$ and $A_t= 205\text{cm}^2$). The distance from the main gate to the end of the apron is 125cm, as shown in Figure 1. Two piers each with length 55cm, made from baseform are fastened at the contraction part with 50 cm length. There are three vertical gates which made from clear Perspex, and slides through vertical grooves. The false bed height is 12 cm and the model height over it equals 48 cm. A movable sand bed of length 9.0m and 0.12m thickness is formed just DS of stilling basin, the geometric mean diameter of movable soil equals to 0.5mm. Details of the tested waterway passage are presented in Table 1. Both symmetric and asymmetric operations of gates were considered. All runs were performed under constant submergence of about 6.0 for a range of the initial Froude number of 2.2 to 5.5. The total number of runs was 139.

Table 1. Models dimensions and corresponding operational scenarios

Model type	$A_o=a_o/A_t$	Remarks
1- $a_o= 0.00$ (solid deflector, $A_t=205\text{ cm}^2$)	0.0	
2- $a_o= 18.5\text{cm}^2$, ($L_1=26.5\text{cm}$, $L_{d1}=1.2\text{cm}$, $L_{d2}=1.2\text{cm}$)	9.5%	1- Opening area in deflector ($L_d= 4.5\text{cm}$, $h_d= 6.0\text{cm}$, $b_d= 30\text{cm}$)
3- $a_o= 39.0\text{cm}^2$, ($L_1=18\text{cm}$, $L_{d1}=1.2\text{cm}$, $L_{d2}=1.2\text{cm}$)	19.0%	2- The total area of the deflector, $A_t= 205\text{cm}^2$
4- $a_o= 57.4\text{cm}^2$, ($L_1=10\text{cm}$, $L_{d1}=1.2\text{cm}$, $L_{d2}=1.2\text{cm}$), $A_o=a_o/A_t=0.28$	28.0%	3- No. of runs = 139
5- $a_o= 76.9\text{cm}^2$, ($L_1=2.2\text{cm}$, $L_{d1}=1.2\text{cm}$, $L_{d2}=1.2\text{cm}$), $A_o=a_o/A_t=0.375$	37.5%	1- A+B+C 2- A+C 3- A+B 4- B 5- A
6- $a_o= 125\text{cm}^2$, ($L_1=2.2\text{cm}$, $L_{d1}=0.7\text{cm}$, $L_{d2}=1.95\text{cm}$), $A_o=a_o/A_t=0.61$	61.0%	

Near-Bed-Velocity Measurements

The near-bed-velocities along the tested models at pre-specified positions were measured using an electromagnetic currentmeter. The meter measures the velocity in two directions, one in the flow direction (v_x) and the other in the lateral direction (v_y). The velocities were measured near the bed by 2 cm along both the rigid and the movable soil as shown in the Figure 3. The velocity vectors were measured at five cross section DS the sudden expanding cross section by 25, 50, 75, 85, 95, and 105cm. In the lateral direction, the velocity vectors were measured at distances 10, 20, and 30cm from the glass side. A point gauge was used to measure the dimensions of scour hole downstream the basin of the multi-vents regulator.



Laboratory Test Procedure

The time taken by each run was estimated to be 50 minutes where about 95% of maximum scour occurs, Negm et al. [15.16]. The following procedure was followed to collect the experimental measurements, (i) The pump was switched on and the required discharge was passed gradually using the discharge control valve; (ii) The required height of the gate opening is adjusted; (iii) The tail gate was adjusted to form submerged jump over the rigid bed; (iv) The movable bed (sandy soil) was re-leveled horizontally with the fixed bed after reaching the equilibrium conditions; (v) The running time of the test was started; (vi) The velocities were measured at the selected sections using the electromagnetic current meter; (vii) After the run time was terminated, (50 minutes), the pump was turned off; (viii) The tail gate was screwed gradually until the channel became empty; (vii) The scour mesh was measured; and (x) The stilling basin model was changed and steps from 1 to 10 were repeated.

RESULTS AND DISCUSSIONS

The collected raw data were converted into dimensionless values according to Eq. (1) and Eq. (2) for all gates operation scenarios including (A+B+C), (A+B), (A+C), B and A. Relationships between the relative maximum scour depth and the initial Froude number as well as those between the near-bed-velocity ratio and the initial Froude number for all gates operations scenarios and for all tested percentages of waterway passage were displayed as shown later.

Operating All Gates

Samples of the above mentioned relationships are shown in Figures 4 and 5 for operating all gates (A+B+C). The measured 2-D near bed velocity pattern and the corresponding scour patterns are plotted for all runs. Samples of these plots for near bed velocity patterns are shown in Figure 6 for different percentages of waterway passage, A_o of (a) 0.0, (b) 9.5%, (c) 19%, (d) 28%, (e) 37.5%, and (f) 61%; at $L_o= 0.06$ with $S= 5.97$ and $F_1= 4.82$.

Inspection of Figure 6 indicates that reverse flow occurs just DS the solid deflector ($A_o=0.0$) over the rigid bed. The intensity of reverse flow decreases as the percentage waterway passage increases and diminishes beyond the value of $A_o=28\%$. The strength of the velocity vector increases as A_o increases beyond $A_o=28\%$. On the other hand, it was observed that the magnitude of the velocities near bed were of higher values for $A_o>28\%$. These observations indicated that the effectiveness of the curved deflector with 28% waterway passage is better than all other tested percentages of waterways passage.

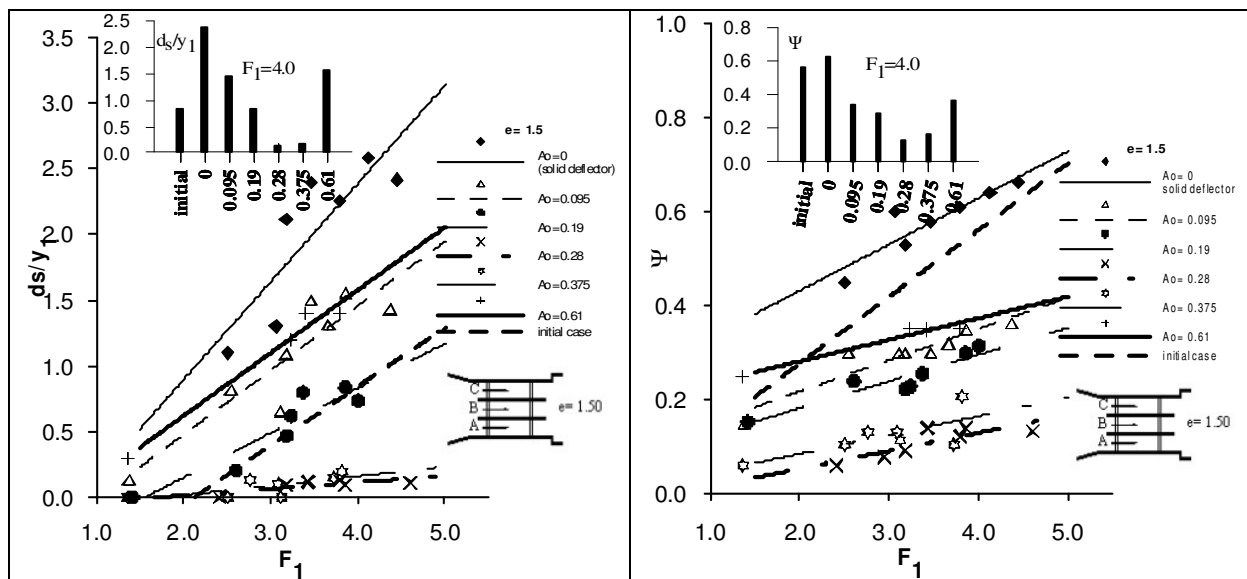
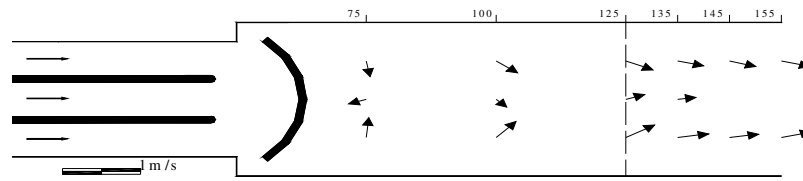
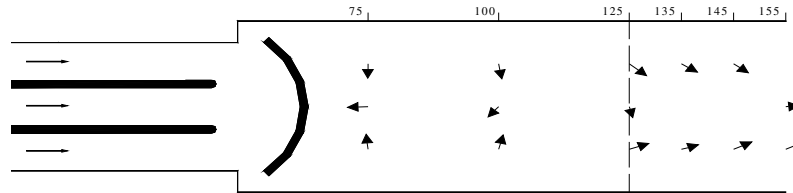


Figure 4. Relationship between ds/y_1 and F_1 for different values of A_o and operating all gates

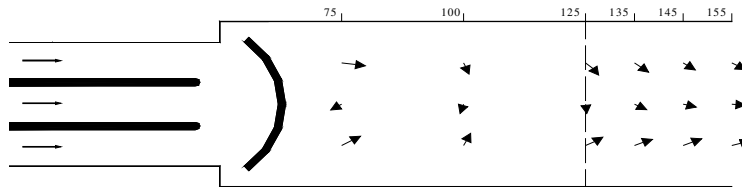
Figure 5. Relationship between ψ and F_1 for different A_o and operating all gates



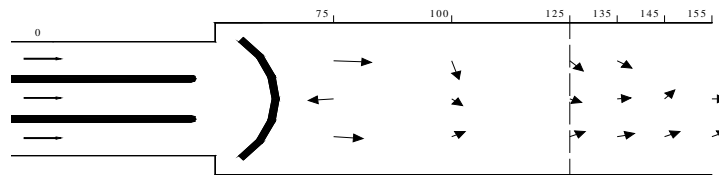
(a) $A_0=0.0$ (solid deflector)



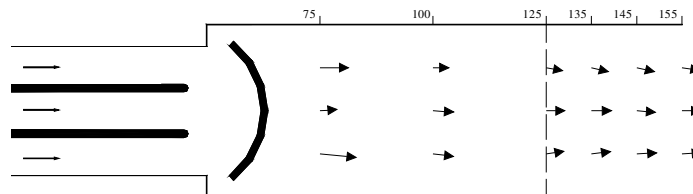
(b) $A_0=9.5\%$



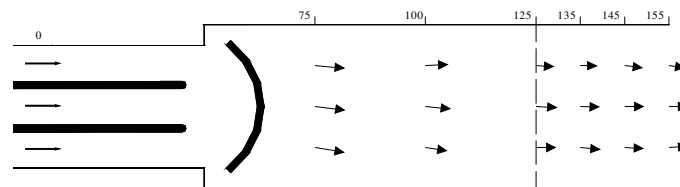
(c) $A_0=19.0\%$



(d) $A_0=28.0\%$



(e) $A_0=37.5\%$



(f) $A_0=61.0\%$

Figure 6. Near-bed-velocity patterns for symmetric operations of three main gates at $L_0=0.06$ with $S=5.97$ and $F_1=4.82$

The relationship presented in Figure 5 indicates the variation of the relative maximum near-bed-velocity with the initial Froude number. This figure shows that the minimum

values of the relative maximum near-bed-velocity (velocity ratio) is obtained at $A_o=28\%$ and the maximum values are obtained when $A_o=0.0$. Other values of A_o produce values of the velocity ratio between the maximum and minimum. These observations confirm those obtained from Figure 6. On the other hand, the relationship presented in Figure 4 indicated that the relative maximum scour depth is minimum at $A_o=28\%$ and maximum at $A_o=0.0$. For all other values of A_o , the values of the scour depth are in between these extremes. These results matched well with those obtained from Figures 5 and 6. Moreover, it is observed that the position of the relative maximum scour depth from the end of the stilling basin is the shortest when using $A_o=28\%$ and the longest ones occur at $A_o=0.0$ while for other A_o ratios, the values L_o are in between. Figure 7 confirms these results.

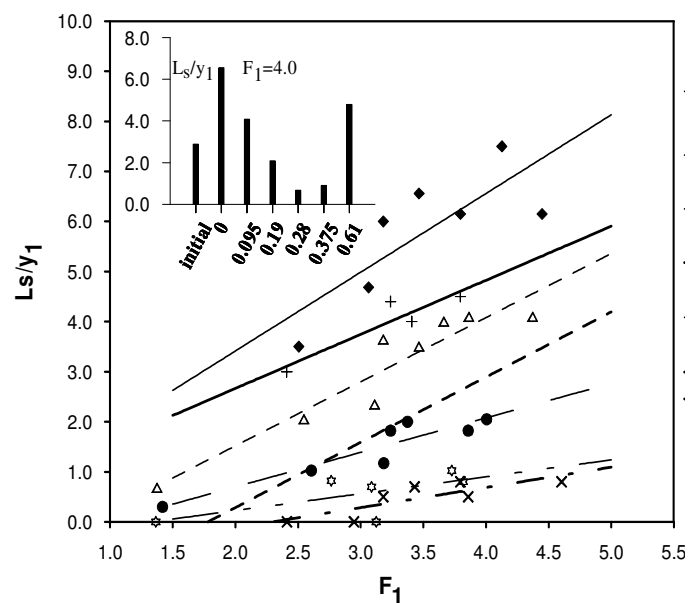


Figure 7. Relationship between L_s/y_1 and F_1 for different values of A_o . (Notions as in Figures 4 and 5)

Operating Two Main Gates

Figures 8 and 9 indicate that the optimal value of A_o is 9.5% when two symmetric gates are operated. The reduction of the maximum relative scour depth reaches about 74% on average at $A_o=9.5\%$. Inspection of Figure 10 indicates that reverse flow occurs just DS the solid deflector ($A_o=0.0$) over the rigid bed. This intensity of reverse flow decreases as the percentage waterway passage increases and diminishes at $A_o=9.5\%$. The strength of the velocity vector increases as A_o becomes more than 9.5% with tendency of minor scale reverse flow over the movable soil. On the other hand, it is observed that the magnitude of the velocities near bed are of higher values for $A_o=0.0$ and decreases with the increase of A_o till it reaches its possible minimum values at $A_o=9.5\%$ or 0.095 and increases again beyond $A_o=9.5\%$.

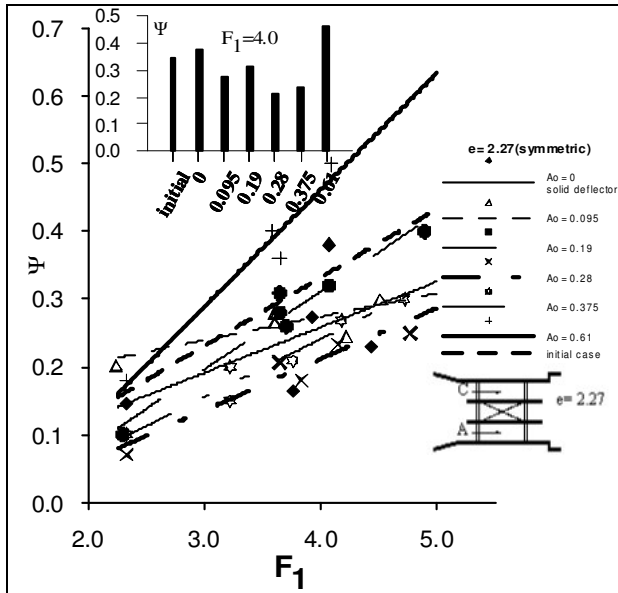


Figure 8. Relationship between y and F_1 for different values of A_0 and operating all gates

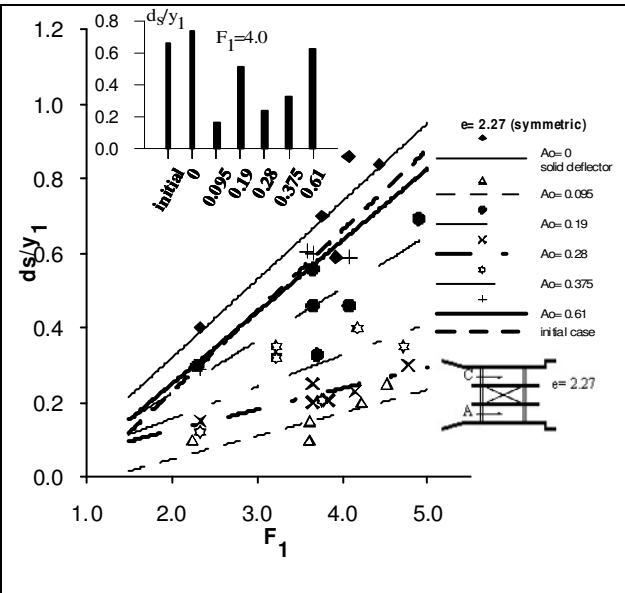
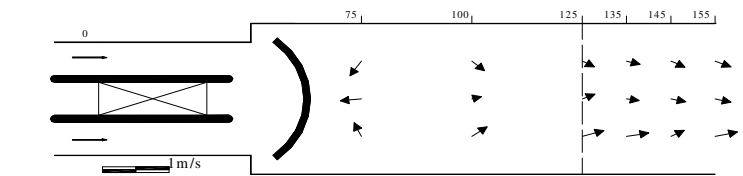
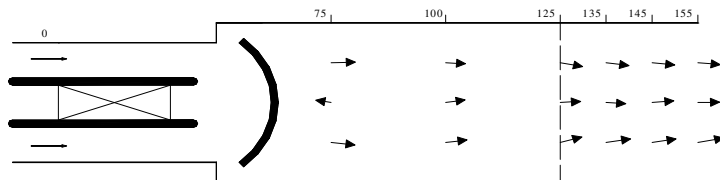


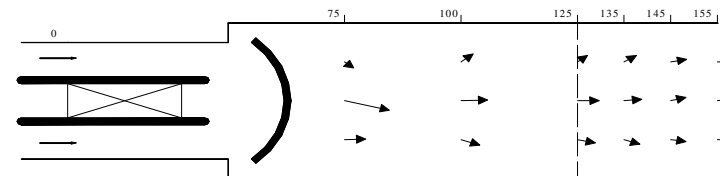
Figure 9. Relationship between ψ and F_1 for different values of A_0 and operating all gates



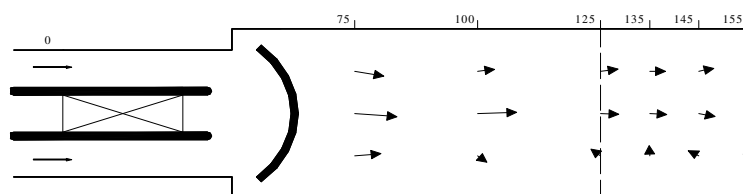
(a) $A_0=0.0$ (solid deflector)



(b) $A_0=9.5\%$



(c) $A_0=19.0\%$



(d) $A_0=28.0\%$

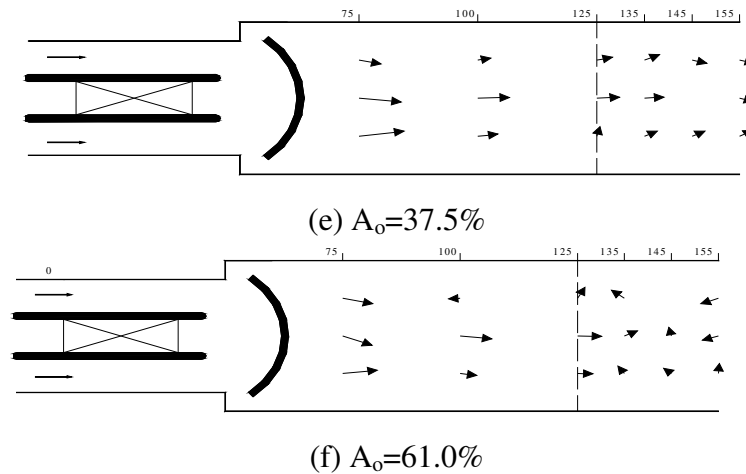


Figure 10. Near bed velocity patterns for symmetric operations of two main gates at $L_o= 0.06$ with $S= 5.97$ and $F_1= 4.82$

Similar Figures (11a and 11b) for asymmetric operations of two gates are analyzed and a ratio of $A_o= 28\%$ resulted in the maximum reduction in both the velocity ratio and the relative maximum scour depth. This reduction reaches about 76% in d_s/y_1 compared to solid deflector ($A_o= 0.0$). Figure 11a shows the relationship between d_s/y_1 and F_1 which confirms the obtained results. While Figure 11b presents the relationship between ω and F_1 for different A_o and operating two gates asymmetrically which confirms the observations obtained from Figure 11a.

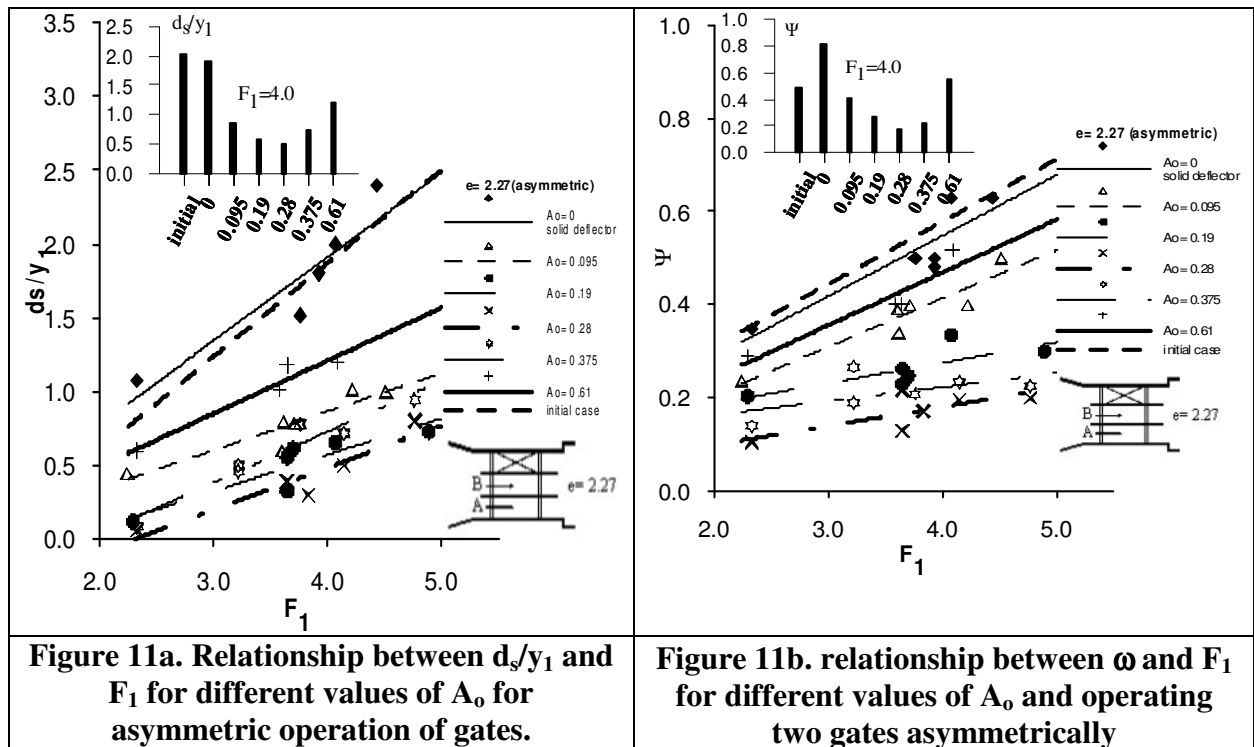


Figure 11a. Relationship between d_s/y_1 and F_1 for different values of A_o for asymmetric operation of gates.

Figure 11b. relationship between ω and F_1 for different values of A_o and operating two gates asymmetrically

Operating Single Main Gate

The flow patterns represented by the near bed velocity for operating symmetric single gate (middle gate) are shown in Figure 12 for different A_o . This figure indicates that the most improved symmetric flow pattern are due to the value of $A_o=28\%$ (or 0.28 on the figure). Also, the magnitude of the velocity vector in this case is minimal.

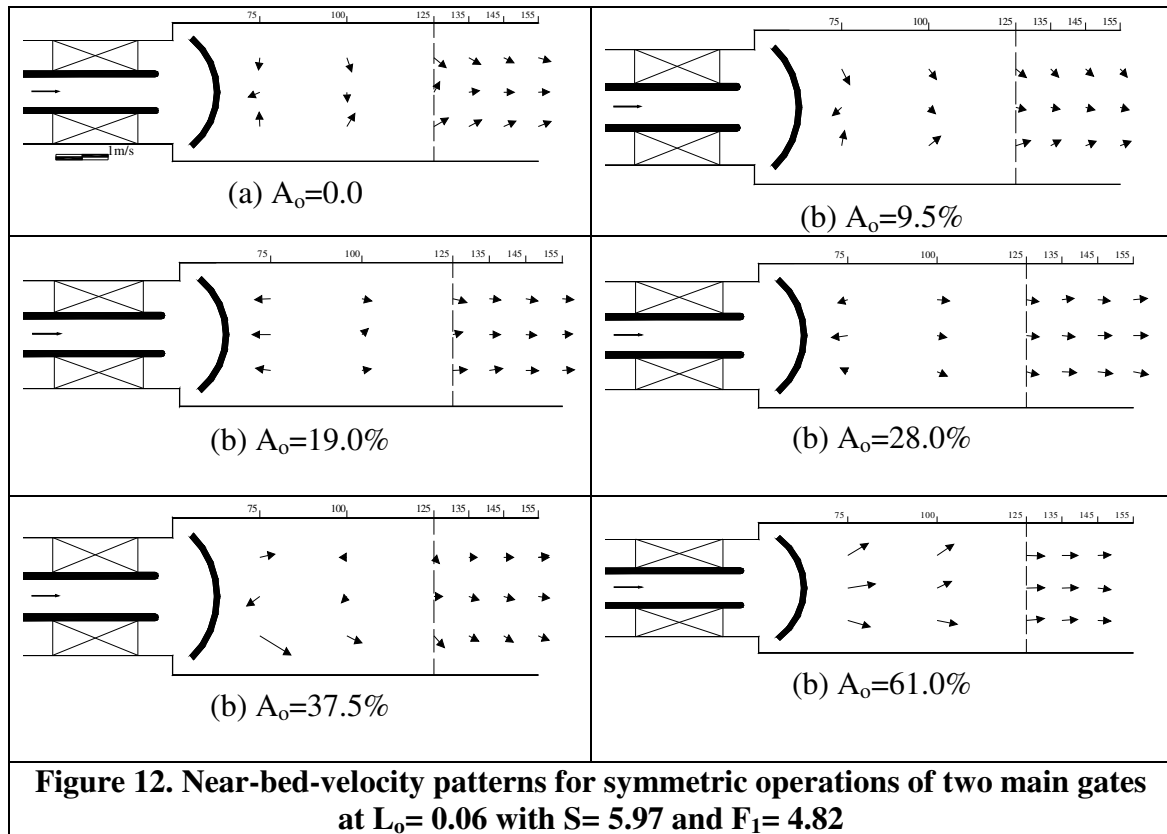


Figure 13 presents the variation of d_s/y_1 versus F_1 for different A_o when only the middle gate (B) is operated (symmetric operation). It is clear that the value of A_o of 28% produces approximately no scour. Also, Figure 13 shows that the same ratio produces minimum values for the velocity ratio. On average conditions, the reduction in d_s/y_1 equals 100% at $A_o=28\%$. For the case of operating single asymmetric gate, the maximum reduction at $A_o=28\%$ is about 82% while it is slightly higher at $A_o=9.5\%$. The flow patterns for these two ratios are presented in Figure 15. Also, Figure 16 shows the relationship between d_s/y_1 and F_1 for different A_o . The figure indicates that both values of $A_o=9.5\%$ and $A_o=28\%$ produce mostly the same reduction in the maximum depth of scour with the priority to the 9.5% due to the difference indicated by the velocity pattern in Figure 15.

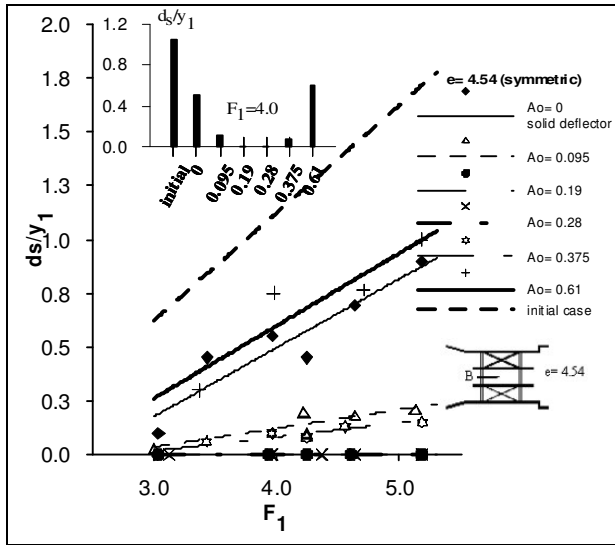


Figure 13. Relationship between d_s/y_1 versus F_1 for different A_o for operating a middle gate

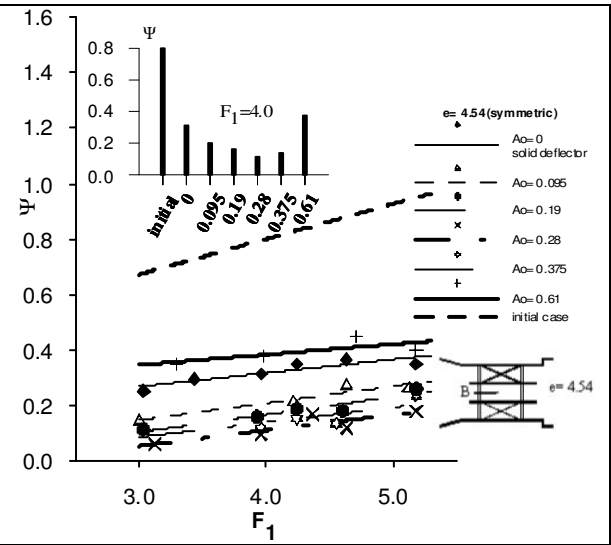


Figure 14. Relationship between ψ versus F_1 for different A_o for operating a middle gate

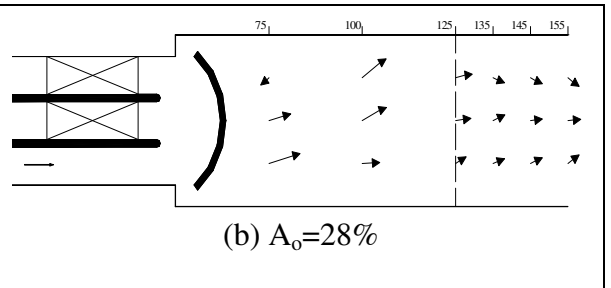
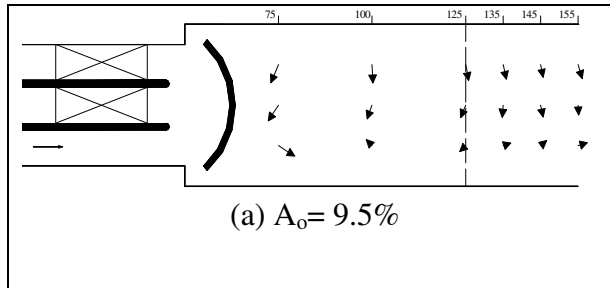


Figure 15. Flow pattern for operating a single asymmetric gate, (a) $A_o=9.5\%$ and (b) $A_o=28\%$.

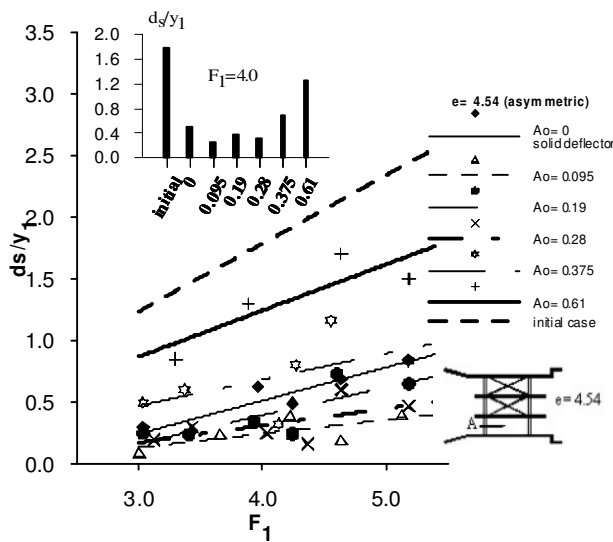


Figure 16. Relationship between d_s/y_1 versus F_1 for different A_o for operating a single asymmetric gate

AVERAGE REDUCTION

Computations based on comparisons of different cases with the case of solid deflector ($A_0=0.0$) indicated that the average reduction in the relative maximum scour depth and the relative maximum near-bed-velocity are as shown in table 2. It should be mentioned here that Negm et al. [17] stated that a reduction of 85% in d_s/y_1 was obtained as a result of using the deflector at the position of $0.06L_b$. Hence the percentage of 28% waterway passage reduces the remaining 15% by about 86%. Numerically, if $d_s/y_1=2.5$ and if y_1 is 0.5 m, then $d_s=1.25$ m. The resulting depth of scour as a result of using a deflector at $0.06L_b$ is $0.15 \times 1.25 = 0.1875$ m which will be reduced to 0.0258 m. For this particular illustrative example, the scour depth will be reduced from 1.25 m to only 2.6 cm which is a great achievement using this kind of new local scour minimizer.

Table 2. Average reduction in d_s/y_1 and in Ψ

TYPE	Percentage reduction due to different $A_0\%$					
	0	9.5	19	28	37.5	61
d_s/y_1	+190	+77	+2	-86	-80	+93
Ψ	+12	-38	-47	-77	-71	-32

CONCLUSIONS

Within the limitations of the present experimental investigation, and from the above analysis and discussions, one could conclude the following:

- i) The relative maximum scour depth d_s/y_1 and the relative near-bed-velocity were increased with the increase of the initial Froude number for all values of waterway passage, A_0 and for all operational scenarios of the gates and vice versa was true.
- ii) Designing the deflector such that it allows the current to be redistributed by making opening through it, helps in reducing significantly the relative near-bed-velocity and hence the resulting relative scour depth was significantly reduced.
- iii) Generally, the best percentage of waterway passage of the curved deflector for minimizing the local scour dimensions and producing symmetric reduced velocity vectors is 28% and located at $0.06L_b$. At this percentage the values of relative near-bed-velocity at the end of stilling basin is minimum and consequently minimum values for relative maximum scour depth were produced.
- iv) The average reduction in the relative maximum scour depth due to the presence of the non-curved deflector is about 86% for operating the three gates at percentage waterway passage of $A_0=28\%$. This reduction is about 75% at $A_0=9.5\%$ for symmetric operations of two gates and about 75% at $A_0=28\%$ for asymmetric operation. When one symmetric gate is operated, no scour appears at $A_0=28\%$ while a reduction of 85% resulted in at $A_0=9.5\%$ for asymmetric operation of one gate.

- v) It is recommended to operate the gates symmetrically and to use 28% opened area in the curved deflector located at $0.06L_b$ in the stilling basin (L_b is the length of the basin).

REFERENCES

1. Abdel Alal, G.M., Modeling of Rectangular Submerged Hydraulic Jumps, *Alexandria Engineering Journal*, Vol. 43, No. 6, 2004, pp. 865-873.
2. Abdel-Gawad, S.M., and McCorquodale, J.A. 1984, Modeling Submerged Radial Hydraulic Jump, Annual Conference Canadian Society for Civil Eng., Publ. By Canadian Society for Civil Eng., Montreal. Canada, Vol. 2, 1984, pp. 711-725.
3. Abouel-Atta, N., Scour Prevention Using a Floor Jets Mechanism, *Civil Engineering Research Magazine*, Faculty of Engineering, Al-Azhar University. Vol. 17, No. 2, February, 1995, pp. 256-268.
4. Ali, N.A. 1995, Scour Prediction at Submerged Pipelines near the Sea Bed, *Bulletin of the Faculty of Engineering*, Faculty of Engineering, Assuit University, Vol. 24, No. 1, July, 1995, pp. 9-16.
5. El Masry, A.A., Influence of A Fully Angled Baffled Floor on Scour behind a Hydraulic Structure, *Mansoura Engineering Journal*, Faculty of Engineering, Mansoura University, Vol. 26, No. 4, December, 2001, pp. 33-44.
6. El-Azizi, I., A Study of Submerged Hydraulic Jump Stilling Basins of Low Head Irrigation Structures, M.Sc. Thesis, Faculty of Engineering, Ain Shams University, Egypt, 1985.
7. Govinda Rao, N.S., and Rajaratnam, N., The Submerged Hydraulic Jump, *Journal of Hydraulic Div.*, Vol.89, No. HY1, 1963, pp. 139-163.
8. Hager, W.H., *Energy Dissipators & Hydraulic Jumps*, Kluwer Academic publication, Dordrecht, The Netherlands, 1992, pp. 151-173.
9. Hassan, N.M.K., and Narayanan, R., Local Scour Downstream of An Apron, *Journal of Hydraulic Engineering*, Vol. 111, No. 11, November, 1986, pp. 1371-1385.
10. Long, D., Steffler, P.M., and Rajaratnam, N., A Numerical Study of Flow Structure in Submerged Jumps, *Journal of Hydraulic Res.*, Vol. 29, No. 3, 1991, pp. 293-307.
11. McCorquodale, J.A., and Khalifa, Abdelkawi M., Submerged Radial Hydraulic Jump, *Journal of the Hydraulics Division*, ASCE, Vol. 106, No. 3, Mar, 1980, pp. 355-367.
12. Mohamed, M.S., Negm, A.M., and El-Saiad, A.A., Effect of Continuous Sill on Scour Downstream Hydraulic Structures, *Civil Engineering Research Magazine*, Faculty of Engineering, Al-Azhar University, Vol. 21, No. 3, July, 1999, pp. 625-645.
13. Narayanan, S., and Bhargara P., Pressure Fluctuations in Submerged Jump, *Journal of the Hydraulic Div.*, Vol. 102, No. HY3, 1976, pp. 339-350.
14. Negm, A.M., Abdel-Aal, G.M., Elfiky, M.I., and Mohamed, Y.A., Characteristics of Submerged Hydraulic Jump in Radial Basins with a Vertical Drop in the Bed, *AEJ*, Faculty of Eng., Alexandria University, Alexandria, Egypt, Vol. 42, No. 1, 2003, pp. 65-76.

15. Negm, A.M., Abdelaal, G.M., Elfiky, M.M. and Abdalla, Y.M., Effects of Multi-Gates Operations on Bottom Velocity Pattern Under Submerged Flow Conditions, Proc. IWTC10 2006, Alexandria, Egypt, March 23-25, Vol. I, 2006, pp. 217-280,
16. Negm, A.M., Abdelaal, G.M., Elfiky, M.M. and Abdalla, Y.M., 2007, Effect of Multi-Gates Regulators Operations on Downstream Scour Pattern Under Submerged Flow Conditions, Proc. IWTC11 2007, Sharm El-Sheikh, Egypt, March 15-18, Vol. II, 2007, pp. 735-767.
17. Negm, A.M., Abdelaal, G.M., Elfiky, M.M. and Abdalla, Y.M., 2008, Optimal Position of Curved Deflector to Minimize Scour Downstream of Multi-Vents Regulators Proc. IWTC12 2008 Alexandria, Egypt, March 27-30, Vol. I, 2008, pp. 1269-1283.
18. Rajaratnam, N., Submerged Hydraulic Jump, Journal of the Hydraulic Div., Vol. 91, No. HY4, 1965, pp. 71-96.
19. Rajaratnam, N., Hydraulic Jump in Advances in Hydro-Science, Vol. 14, Edited by V.T. Chow, Academic Press, New York and London, Academic Press, New York and London, 1967, pp. 197-280.
20. Saleh, O.K., Negm, Ahmed, N.G., Effect of Asymmetric Side Sill on Scour Characteristics Downstream of Sudden Expanding Stilling Basins, Proc. of 6th Int. Conf. on Hydro-Science and Engineering, 30 May - 4 June, 2004, Cairns, Australia, ICHE2004, 2004.
21. Zidan, A.R., Owais, T.M., Abdel-Motaim M., and El-Masry, A., Scour Behind Sluice Gates, Mansoura Engineering Journal, Faculty of Engineering, Mansoura University, Vol. 8, No. 2, December, 1983, pp. 1-19.

NOMENCLATURES

- A_o : The ratio of the area a_o to A_t , [-]
- A_t : The total surface area of the curved deflector, [L^2].
- a_o : The opening areas in the curved deflector, [L^2].
- B : The flume width, [L].
- B_o : The relative width of the curved deflector (b_d/B), [-].
- b_d : The width of the deflector, [L].
- b_e : The width DS the working gates [L].
- d_{50} : The mean diameter of the sand base, [L].
- F_1 : Froude number at the vena contracta
- g : The gravitational acceleration, [LT^{-2}].
- h_d : The deflector height, [L].
- L : The basin length DS sudden expanding cross section, [L].
- L_d : The distance from the beginning of sudden expanding cross section to the curved deflector, [L].
- L_o : The relative position of the curved deflector, [L_d/L].
- S : The submergence ratio (y_t/y_1), [-].
- v_1 : The velocity at the supercritical flow depth y_1 , [LT^{-1}].
- v_b : The maximum near-bed velocity measured at the end of the basin, [LT^{-1}].

- w: The pier width, [L].
- y_1 : The supercritical flow depth, [L].
- y_t : The tail water depth, [L].
- ϕ : The deflector angle, [-].
- μ : The dynamic viscosity of water, [ML⁻¹T⁻¹].
- ρ_s : The density of sand particles, [ML⁻³].
- ρ : The density of water, [ML⁻³].
- ω : The scenario of operating gates systems, [-].